

Supplementary Information

Characteristics of Microcontact Printing with Polyelectrolyte Ink for the Precise Preparation of Patches on Silica Particles

Marc Zimmermann,^{ab} Dmitry Grigoriev,^a Nikolay Puretskiy^a and Alexander Böker^{*ab}

^a. Fraunhofer Institute for Applied Polymer Research IAP, D-14476 Potsdam-Golm, Germany. E-mail: marc.zimmermann@iap.fraunhofer.de

^b. Chair of Polymer Materials and Polymer Technologies, University Potsdam, D-14476 Potsdam-Golm, Germany

Table of Contents

Tables with Measured Values	2
Fluorescence and Scanning Electron Microscope	4
Single Patched Particles (SPP)	4
Double Patched Particles (DPP).....	8
Scanning Force Microscopy	12
Single Patched Particles (SPP)	12
Double Patched Particles (DPP).....	15
Influence of Particle Size Distribution on Patch Diameter	18
Electrostatic Bonding: pH Dependence.....	20
Influence of Particle Size on Printing Pressure.....	21

Tables with Measured Values

All measured values, which are graphically displayed in the main article, can be found below: patch diameter d for single and double patched particles (SPP & DPP), surface area of patch A_f , ratio between larger and smaller patch R for DPP and influence of particle size distribution on patch diameter e . Additionally the patchy particle yield Y for SPP and DPP

Table S1 Patch diameter d with standard deviation for single patched particles (SPP) at different particle sizes and increasing polymer ink concentration. Results were obtained using fluorescence microscopy and measuring the patches in different samples.

PEI [wt%]	$d_{5\mu\text{m}}$ [μm]	$d_{4\mu\text{m}}$ [μm]	$d_{2\mu\text{m}}$ [μm]	$d_{1\mu\text{m}}$ [μm]
1	1.80 ± 0.22	1.72 ± 0.17	1.13 ± 0.15	0.59 ± 0.08
2	2.16 ± 0.29	2.00 ± 0.20	1.20 ± 0.15	
3	2.38 ± 0.31	2.23 ± 0.25		
4	2.57 ± 0.32			

Table S2 Patch thickness t with standard deviation for single patched particles (SPP) at different particle sizes and increasing polymer ink concentration. Results were obtained by indirect measurement of the dried PDMS stamps after particle release using SFM.

PEI [wt%]	$t_{5\mu\text{m}}$ [nm]	$t_{4\mu\text{m}}$ [nm]	$t_{2\mu\text{m}}$ [nm]	$t_{1\mu\text{m}}$ [nm]
1	23 ± 6	14 ± 1	11 ± 4	8 ± 2
2	48 ± 5	29 ± 6	19 ± 5	
3	82 ± 4	62 ± 9		
4	125 ± 8			

Table S3 Patch surface area as a fraction of the total particle surface A_f for single patched particles (SPP) at different particle sizes and increasing polymer ink concentration. Additionally, the size ratio R between larger and smaller patches on double patched particles (DPP) was also calculated for all particle sizes and higher polymer ink concentration.

PEI [wt%]	$A_{f_{5\mu\text{m}}}$ [%]	$A_{f_{4\mu\text{m}}}$ [%]	$A_{f_{2\mu\text{m}}}$ [%]	$A_{f_{1\mu\text{m}}}$ [%]	$R_{5\mu\text{m}}$	$R_{4\mu\text{m}}$	$R_{2\mu\text{m}}$	$R_{1\mu\text{m}}$
1	3.2	4.6	8.0	8.6	1.12	1.14	1.14	1.11
2	4.7	6.3	9.0		1.13	1.16	1.22	
3	5.7	7.8			1.16	1.31		
4	6.6				1.27			

Table S4 Calculated error e showing the influence of the natural patch size distribution for different particles sizes on the theoretical patch diameter, which was obtained using our simple mathematical model.

PEI [wt%]	$e_{5\mu\text{m}}$ [μm]	$e_{4\mu\text{m}}$ [μm]	$e_{2\mu\text{m}}$ [μm]	$e_{1\mu\text{m}}$ [μm]
1	0.13	0.04	0.03	0.07
2	0.18	0.08	0.04	
3	0.23	0.12		
4	0.28			

Table S5 Patch diameter d with standard deviation for double patched particles (DPP) at different particle sizes and increasing polymer ink concentration. Results were obtained using fluorescence microscopy and measuring the patches in different samples.

PEI [wt%]	$d_{5\mu\text{m}}$ [μm]	$d_{4\mu\text{m}}$ [μm]	$d_{2\mu\text{m}}$ [μm]	$d_{1\mu\text{m}}$ [μm]
1	1.96 ± 0.25	1.72 ± 0.25	1.01 ± 0.11	0.50 ± 0.07
2	2.30 ± 0.25	1.84 ± 0.26	1.18 ± 0.18	
3	2.45 ± 0.31	2.23 ± 0.39		
4	2.37 ± 0.45			

Table S6 Patch thickness t with standard deviation for double patched particles (DPP) at different particle sizes and increasing polymer ink concentration. Results were obtained by indirect measurement of the dried PDMS stamps after particle release using SFM.

PEI [wt%]	$t_{5\mu\text{m}}$ [nm]	$t_{4\mu\text{m}}$ [nm]	$t_{2\mu\text{m}}$ [nm]
1	17 ± 5	8 ± 6	16 ± 5
2	26 ± 5	19 ± 4	22 ± 12
3	33 ± 4	29 ± 9	
4	87 ± 7		

Table S7 Table shows the yield Y for single and double patched particles for different printing parameters. Yield for SPP was calculated by counting only clearly visible and correctly functionalized particles with a single patch. Yield for DPP is divided into two numbers: First number resembles clearly visible and correctly functionalized particles with two patches and second number resembles clearly visible and correctly functionalized particles with at least one patch.

Type	PEI [wt%]	$Y_{5\mu\text{m}}$ [%]	$Y_{4\mu\text{m}}$ [%]	$Y_{2\mu\text{m}}$ [%]
SPP	1	86	98	87
SPP	2	90	93	86
SPP	3	88	86	
SPP	4	91		
DPP	1	69 (96)	98(100)	73 (91)
DPP	2	81 (97)	78 (93)	70 (94)
DPP	3	57 (86)	79 (100)	
DPP	4	72 (92)		

Fluorescence and Scanning Electron Microscope

Below microscopic images for all SPP and DPP are displayed. Starting with the single patched followed by the double patched particles, fluorescence and scanning electron microscope images with increasing polyethyleneimine concentrations are shown in Fig. S1 – 4 and Fig. S5 – 8 respectively. Labelling and characterization methods are explained in the “Material and Methods” section above.

Single Patched Particles (SPP)

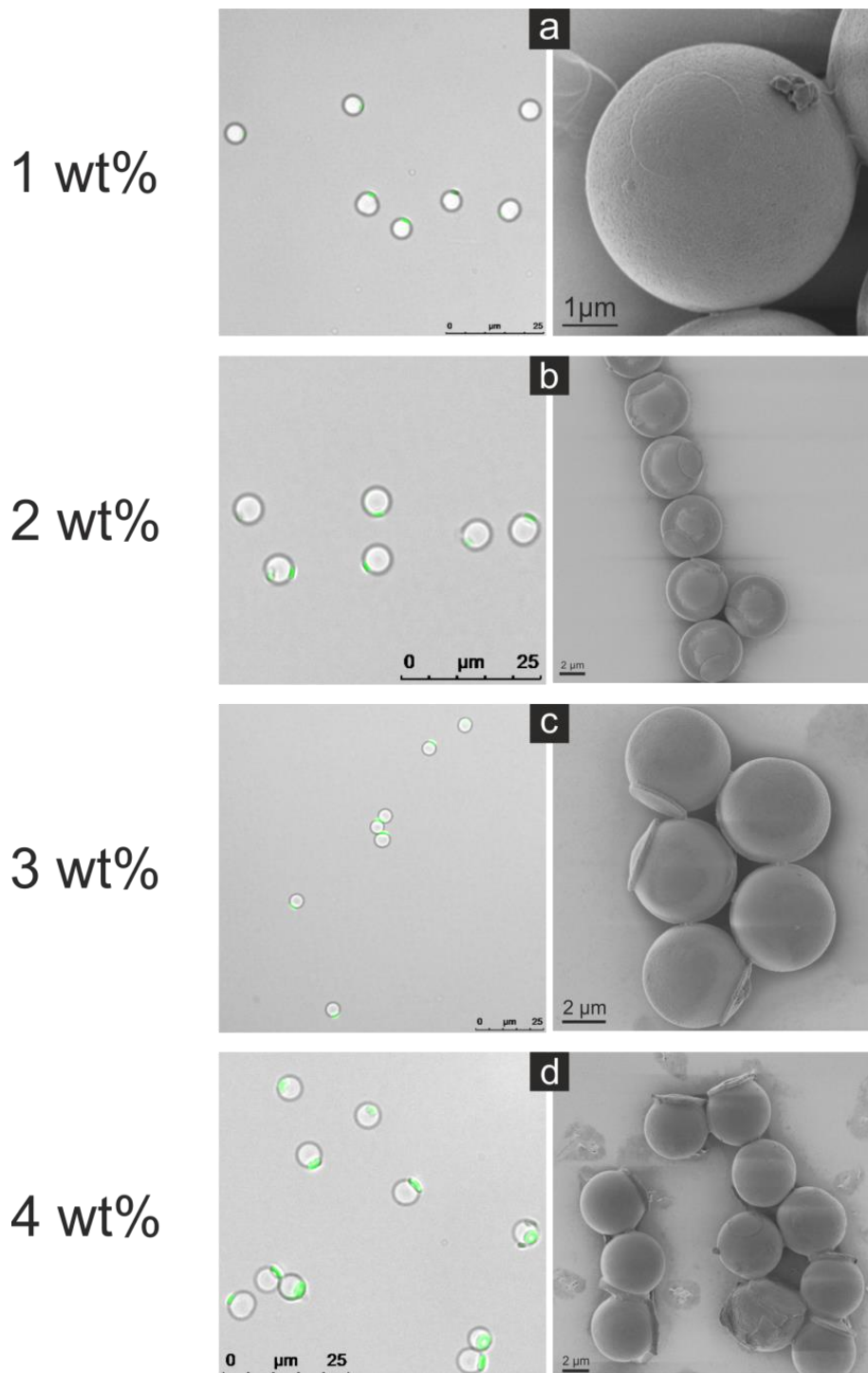
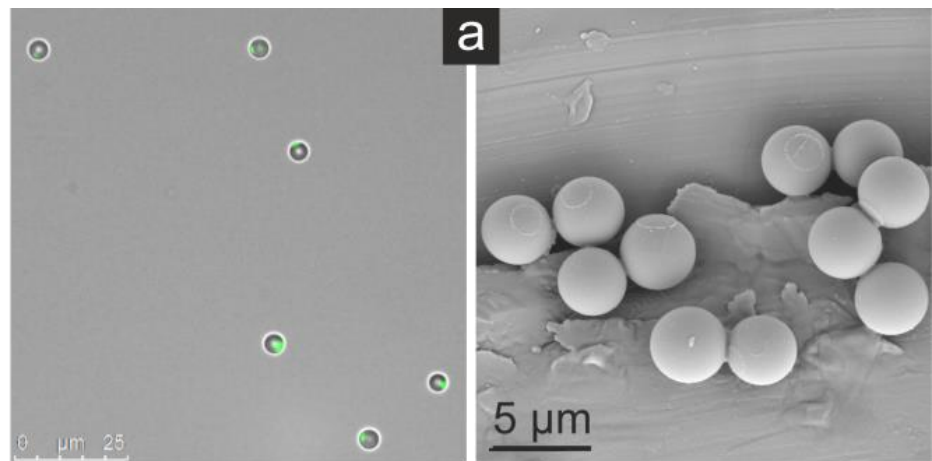
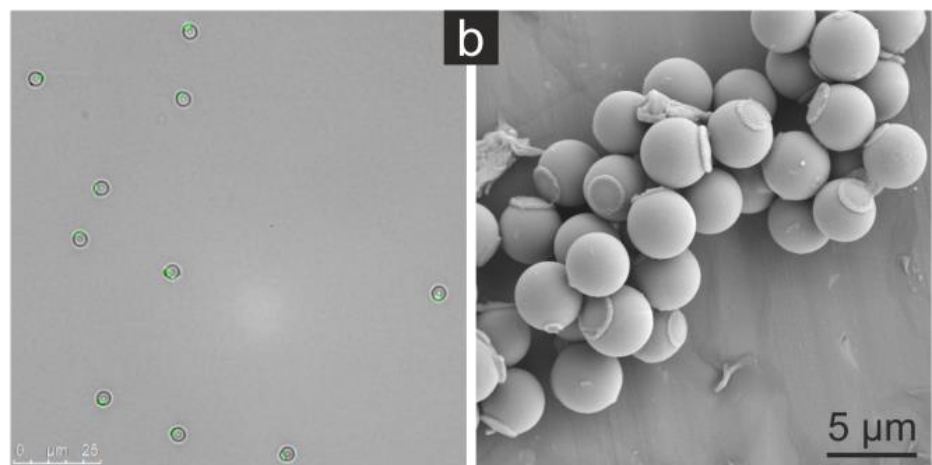


Figure S1 (a – d) Fluorescence microscope and SEM images of 5 μm SPP at increasing PEI concentration (1, 2, 3, and 4 wt%) leading to larger and thicker patches. FM images were obtained by labelling the PEI patches with FITC. SEM samples were sputtered with a 4 nm thick platinum layer prior to measurement.

1 wt%



2 wt%



3 wt%

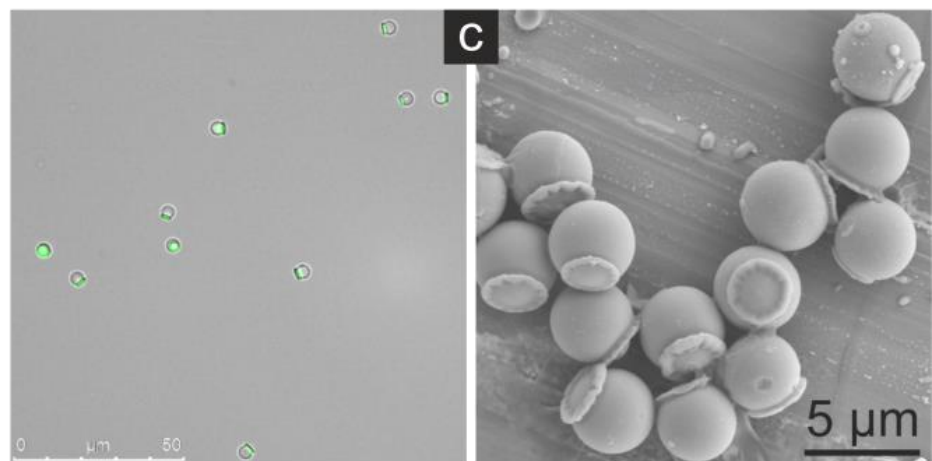


Figure S2 (a – c) Fluorescence microscope and SEM images of 4 μm SPP at increasing PEI concentration (1, 2, and 3 wt%) leading to larger and thicker patches. FM images were obtained by labelling the PEI patches with FITC. SEM samples were sputtered with a 4 nm thick platinum layer prior to measurement.

1 wt%

2 wt%

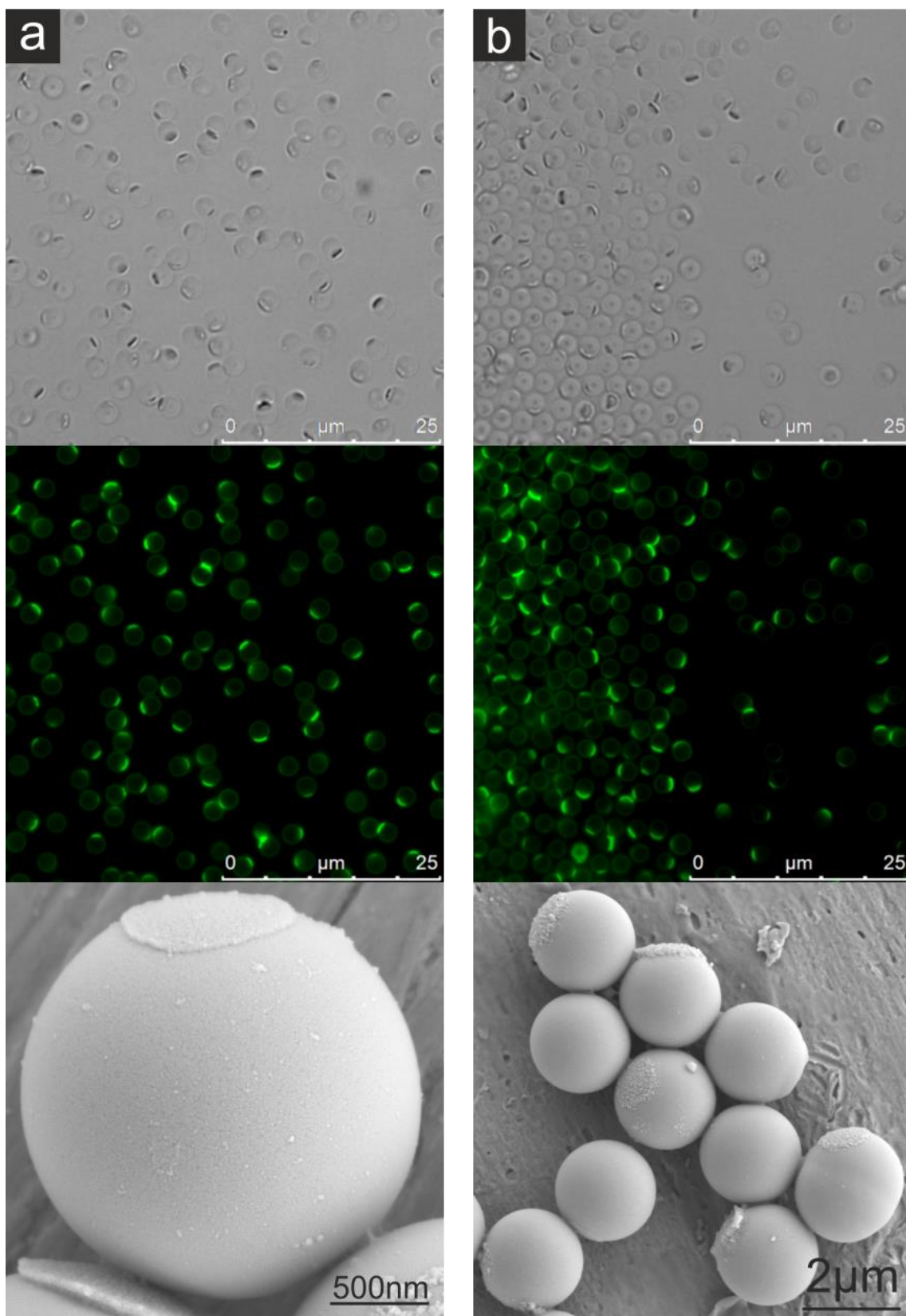


Figure S3 (a - b) Microscope, fluorescence microscope and SEM images of 2 μm SPP at two PEI concentrations (1 and 2 wt%) leading to larger and thicker patches. FM images were obtained by labelling the PEI patches with FITC. SEM samples were sputtered with a 4 nm thick platinum layer prior to measurement.

1 wt%

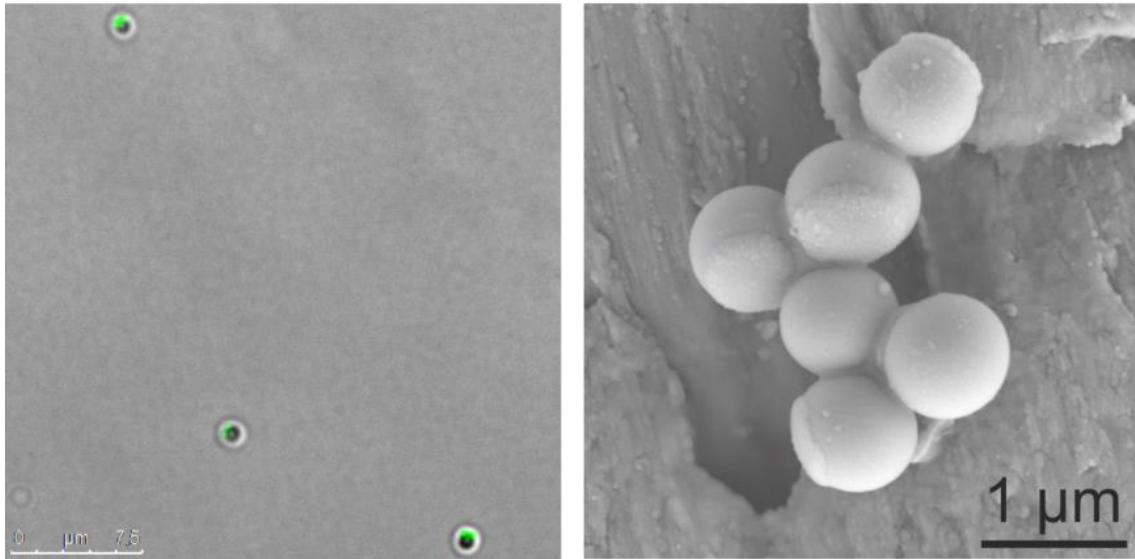
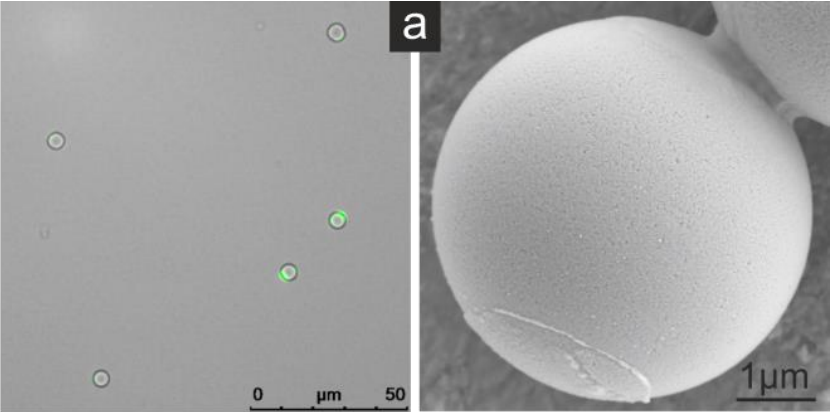


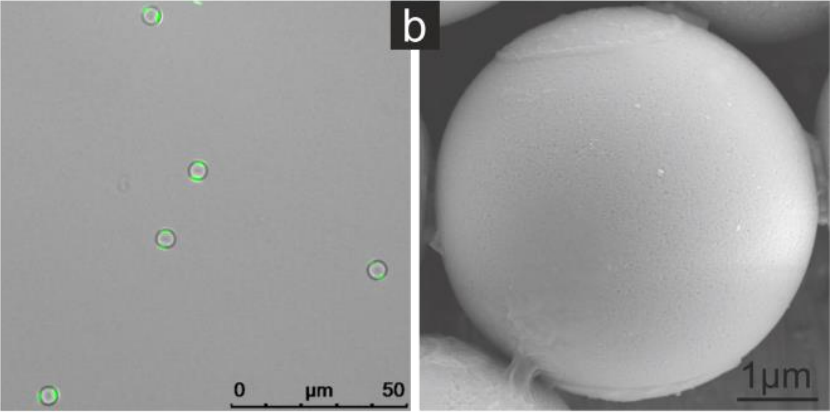
Figure S4 Fluorescence microscope and SEM images of 1 μm SPP printed with a 1 wt% PEI film. FM images were obtained by labelling the PEI patches with FITC. SEM samples were sputtered with a 4 nm thick platinum layer prior to measurement.

Double Patched Particles (DPP)

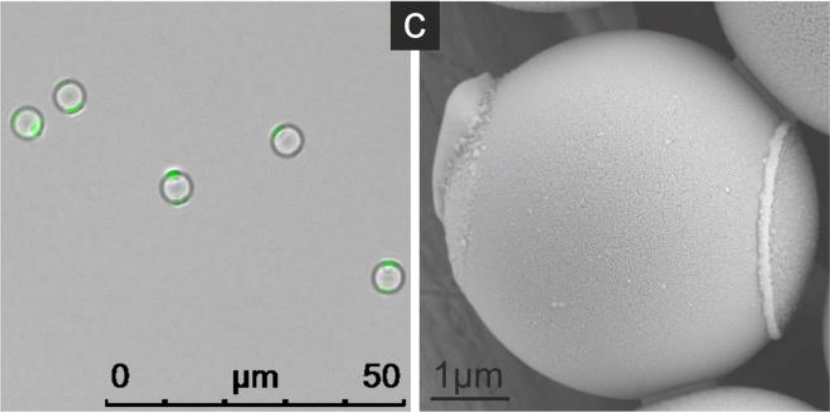
1 wt%



2 wt%



3 wt%



4 wt%

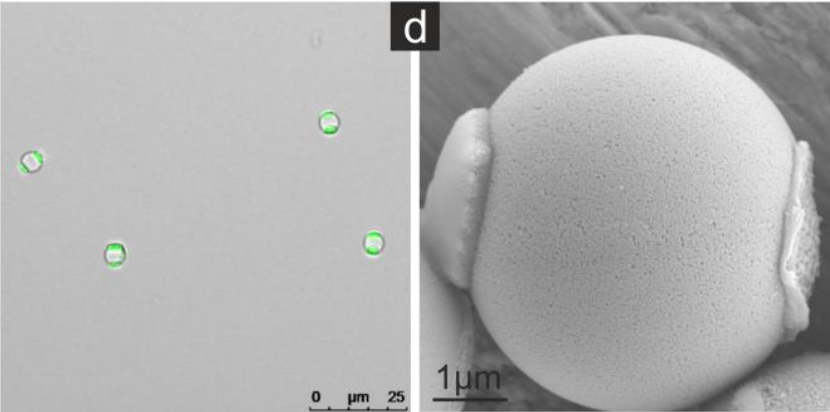
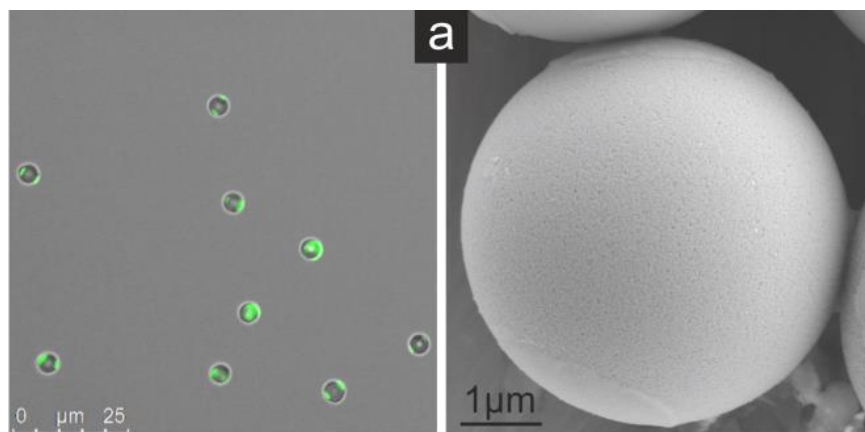
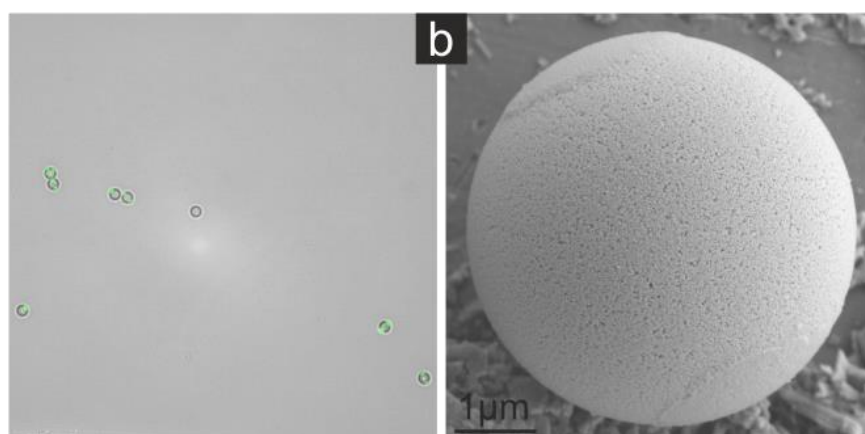


Figure S5 (a – d) Fluorescence microscope and SEM images of 5 μm DPP at increasing PEI concentration (1, 2, 3, and 4 wt%) leading to larger and thicker patches. FM images were obtained by labelling the PEI patches with FITC. SEM samples were sputtered with a 4 nm thick platinum layer prior to measurement.

1 wt%



2 wt%



3 wt%

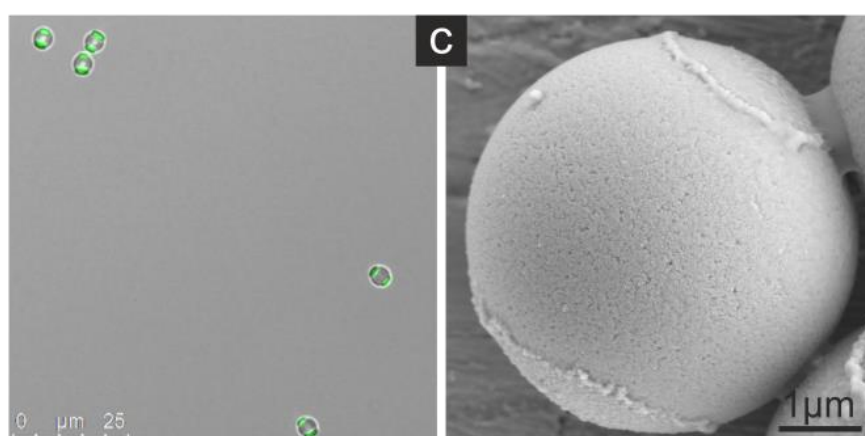


Figure S6 (a – c) Fluorescence microscope and SEM images of 4 μm DPP at increasing PEI concentration (1, 2, and 3 wt%) leading to larger and thicker patches. FM images were obtained by labelling the PEI patches with FITC. SEM samples were sputtered with a 4 nm thick platinum layer prior to measurement.

1 wt%

2 wt%

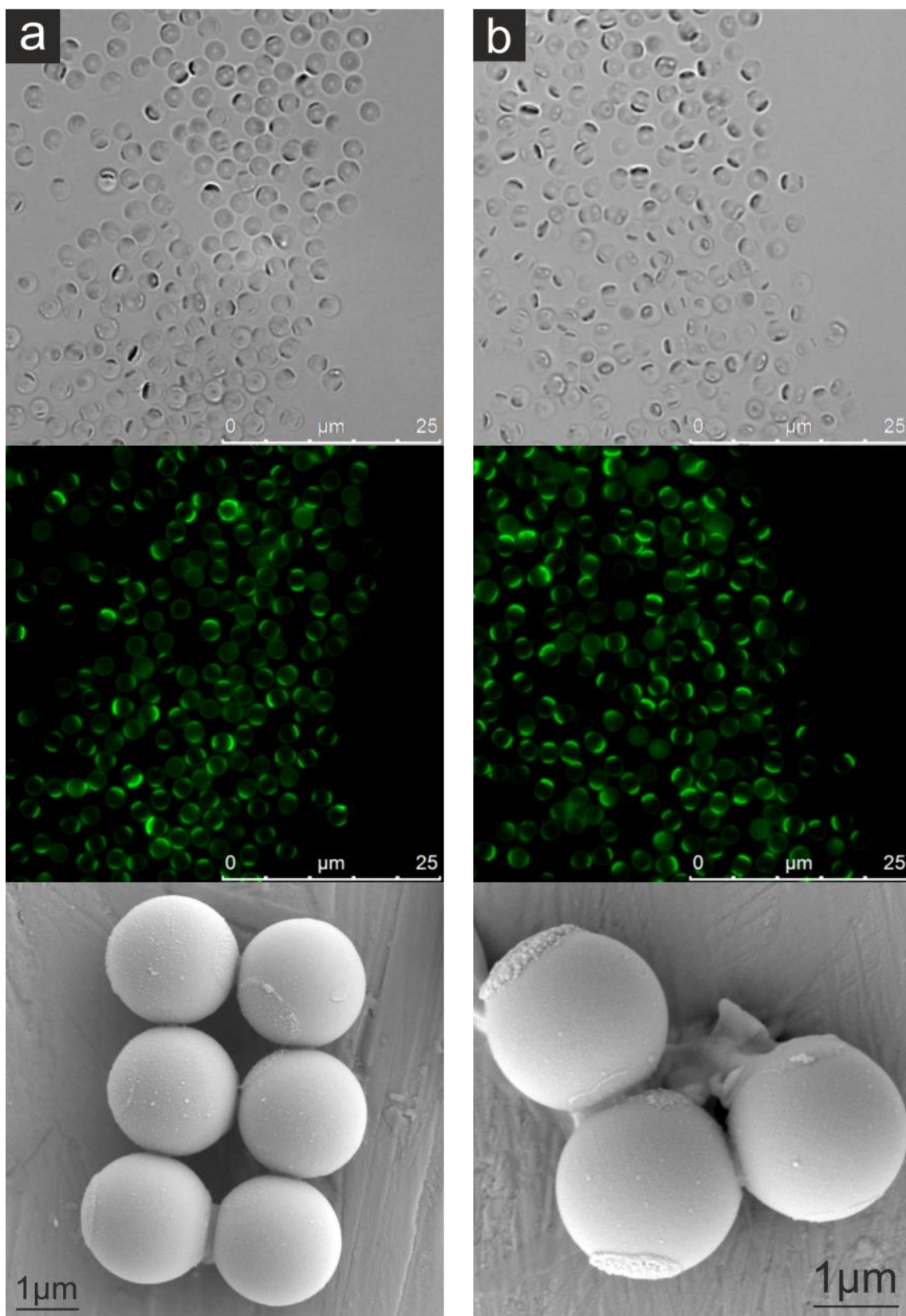


Figure S7 (a - b) Microscope, fluorescence microscope and SEM images of 2 μm DPP at two PEI concentrations (1 and 2 wt%) leading to larger and thicker patches. FM images were obtained by labelling the PEI patches with FITC. SEM samples were sputtered with a 4 nm thick platinum layer prior to measurement.

1 wt%

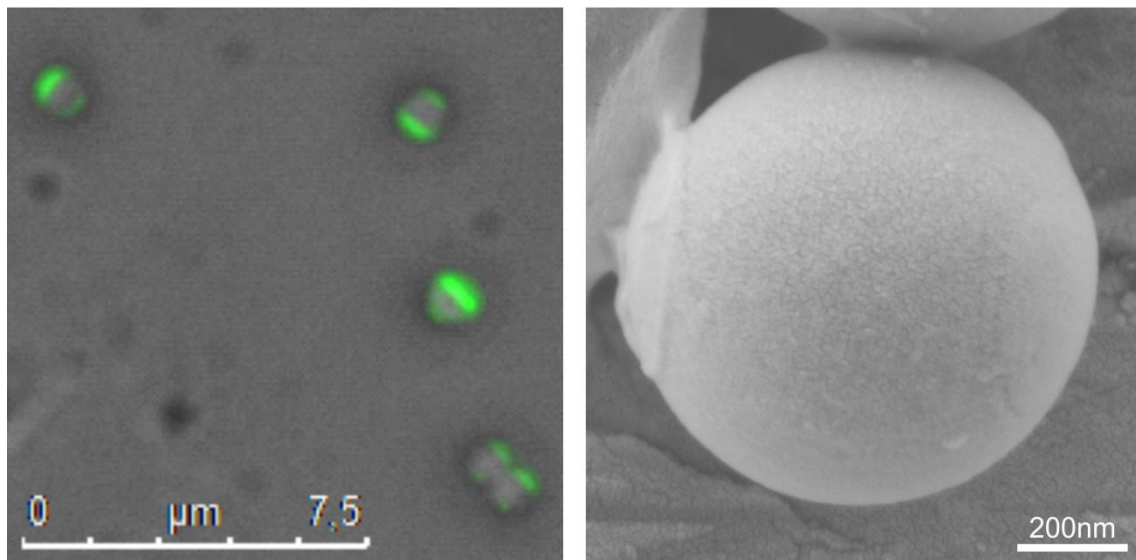


Figure S8 Fluorescence microscope and SEM images of 1 μm DPP printed with a 1 wt% PEI film. FM images were obtained by labelling the PEI patches with FITC. SEM samples were sputtered with a 4 nm thick platinum layer prior to measurement.

Scanning Force Microscopy

Below scanning force microscopy images of the PDMS stamps after particle release for all SPP and DPP are displayed. Starting with the single patched followed by the double patched samples, stamps with increasing polyethyleneimine concentrations are shown in Fig. S9 – 12 and Fig. S13 – 16. PDMS stamps were dried at ambient conditions prior to measurement.

Single Patched Particles (SPP)

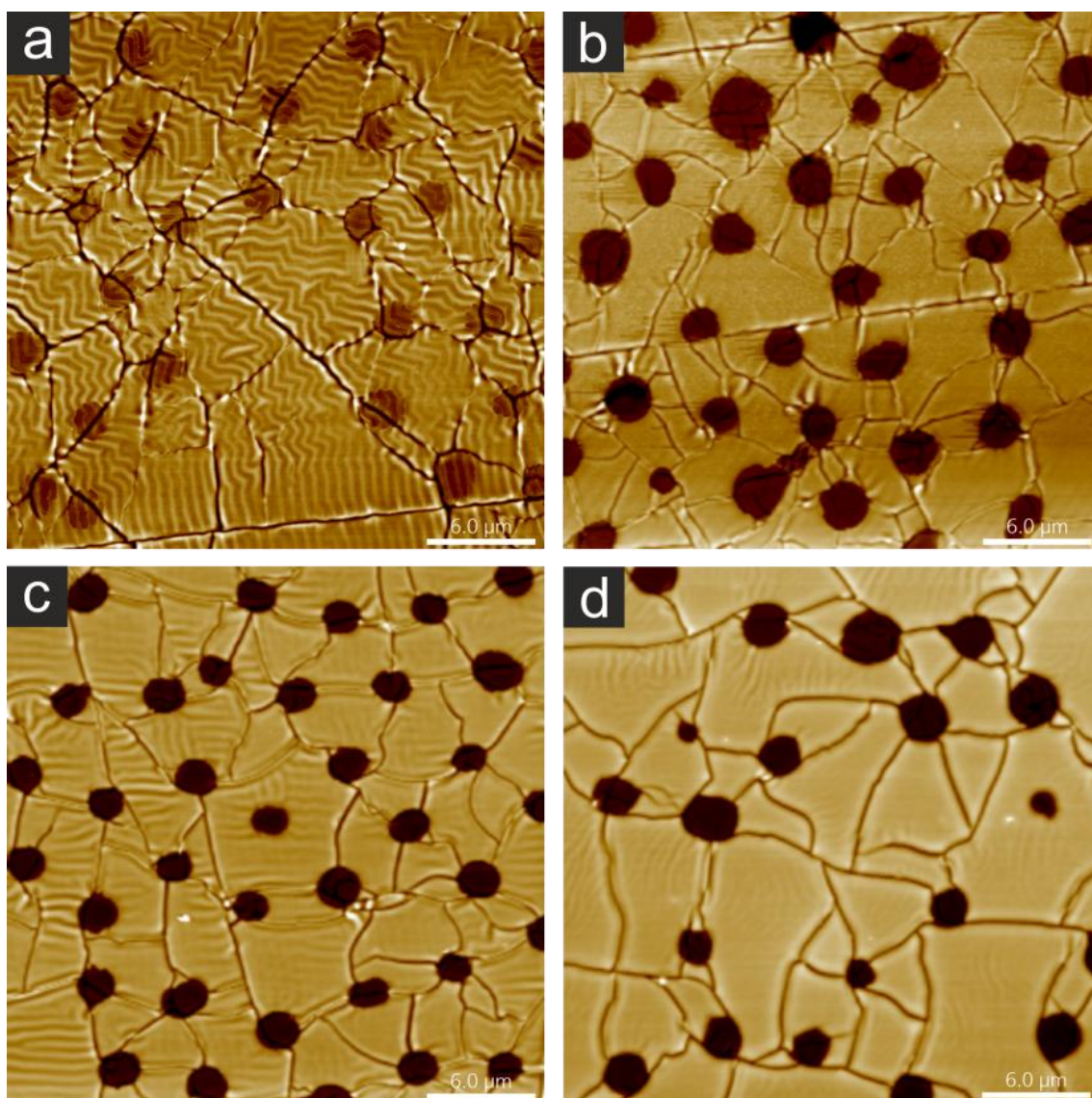


Figure S9 SFM images with a size of $(30 \times 30) \mu\text{m}^2$ of PDMS stamps after $5 \mu\text{m}$ SPP release: a) 1 wt% PEI - Height Scale 80 nm. b) 2 wt% PEI - Height Scale 130 nm. c) 3 wt% PEI - Height Scale 170 nm. d) 4 wt% PEI - Height Scale 230 nm.

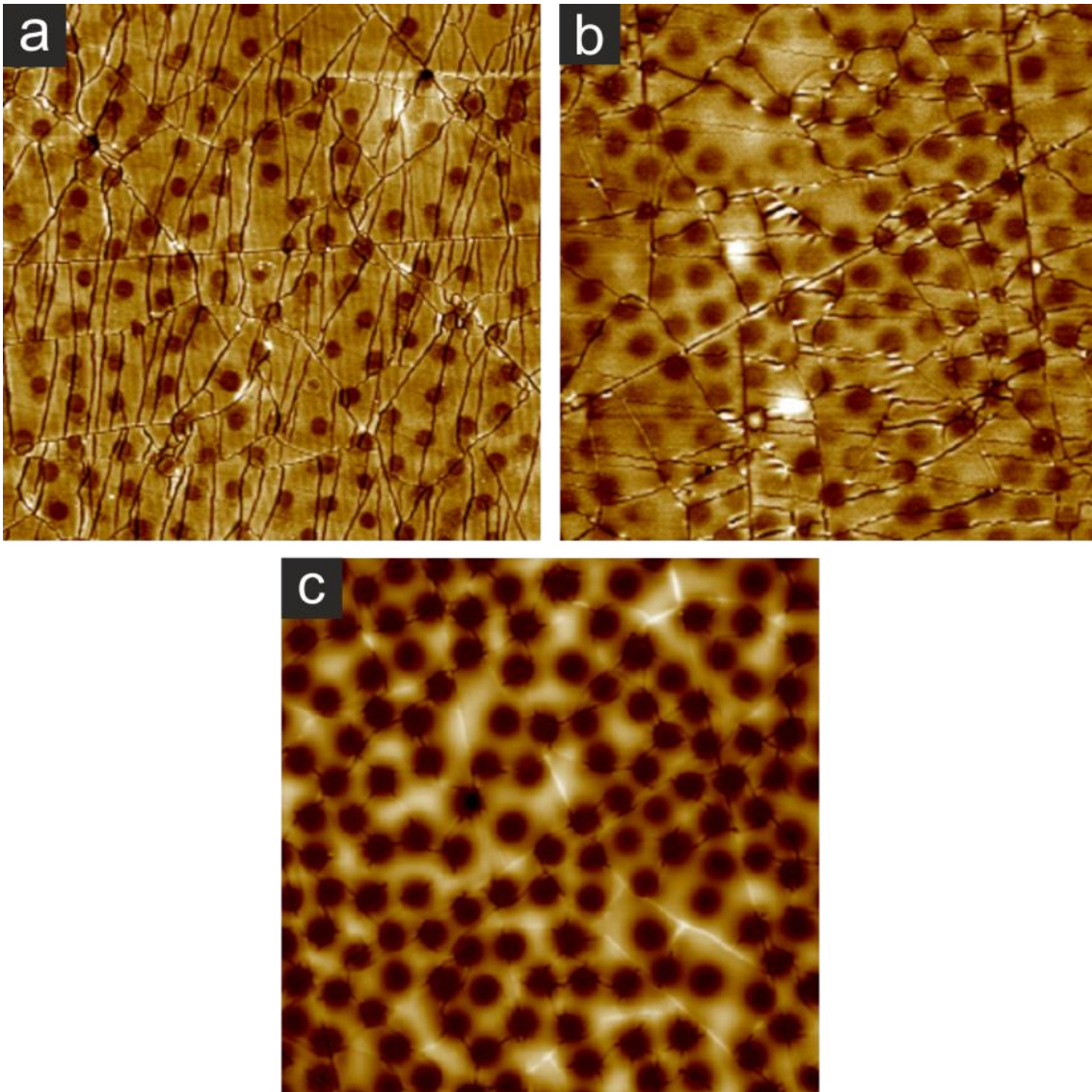


Figure S10 SFM images with a size of $(50 \times 50) \mu\text{m}^2$ of PDMS stamps after $4 \mu\text{m}$ SPP release: a) 1 wt% PEI - Height Scale 50 nm. b) 2 wt% PEI - Height Scale 85 nm. c) 3 wt% PEI - Height Scale 160 nm.

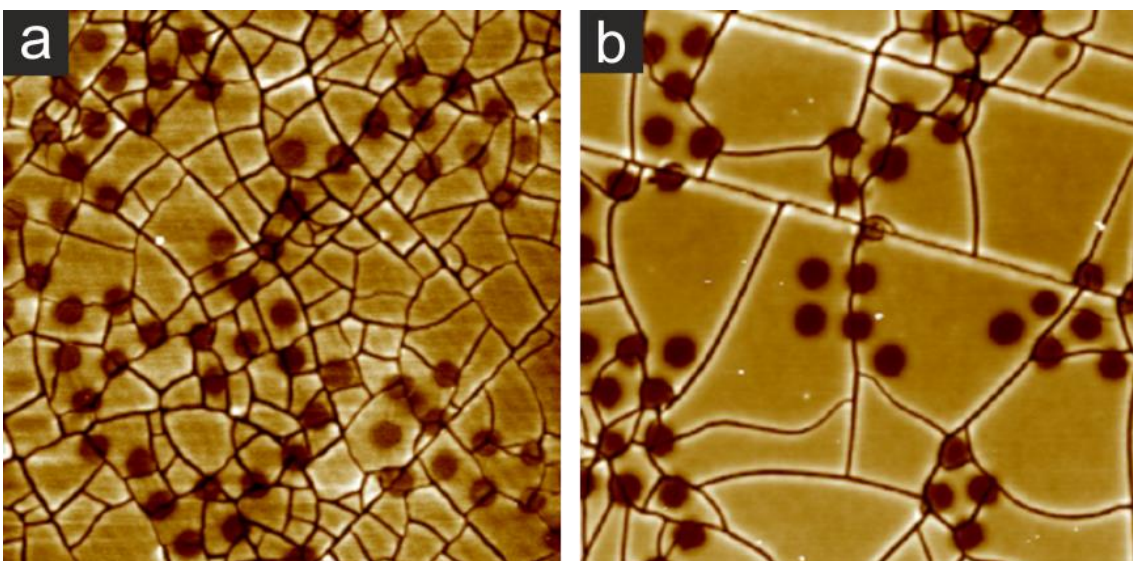


Figure S11 SFM images with a size of $(25 \times 25) \mu\text{m}^2$ of PDMS stamps after $2 \mu\text{m}$ SPP release: a) 1 wt% PEI - Height Scale 50 nm. b) 2 wt% PEI - Height Scale 70 nm.

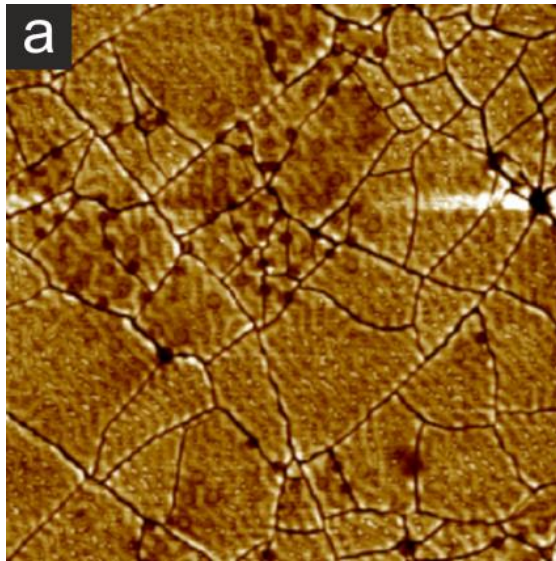


Figure S12 SFM images with a size of $(25 \times 25) \mu\text{m}^2$ of PDMS stamps after $1 \mu\text{m}$ SPP release: a) 1 wt% PEI - Height Scale 50 nm.

Double Patched Particles (DPP)

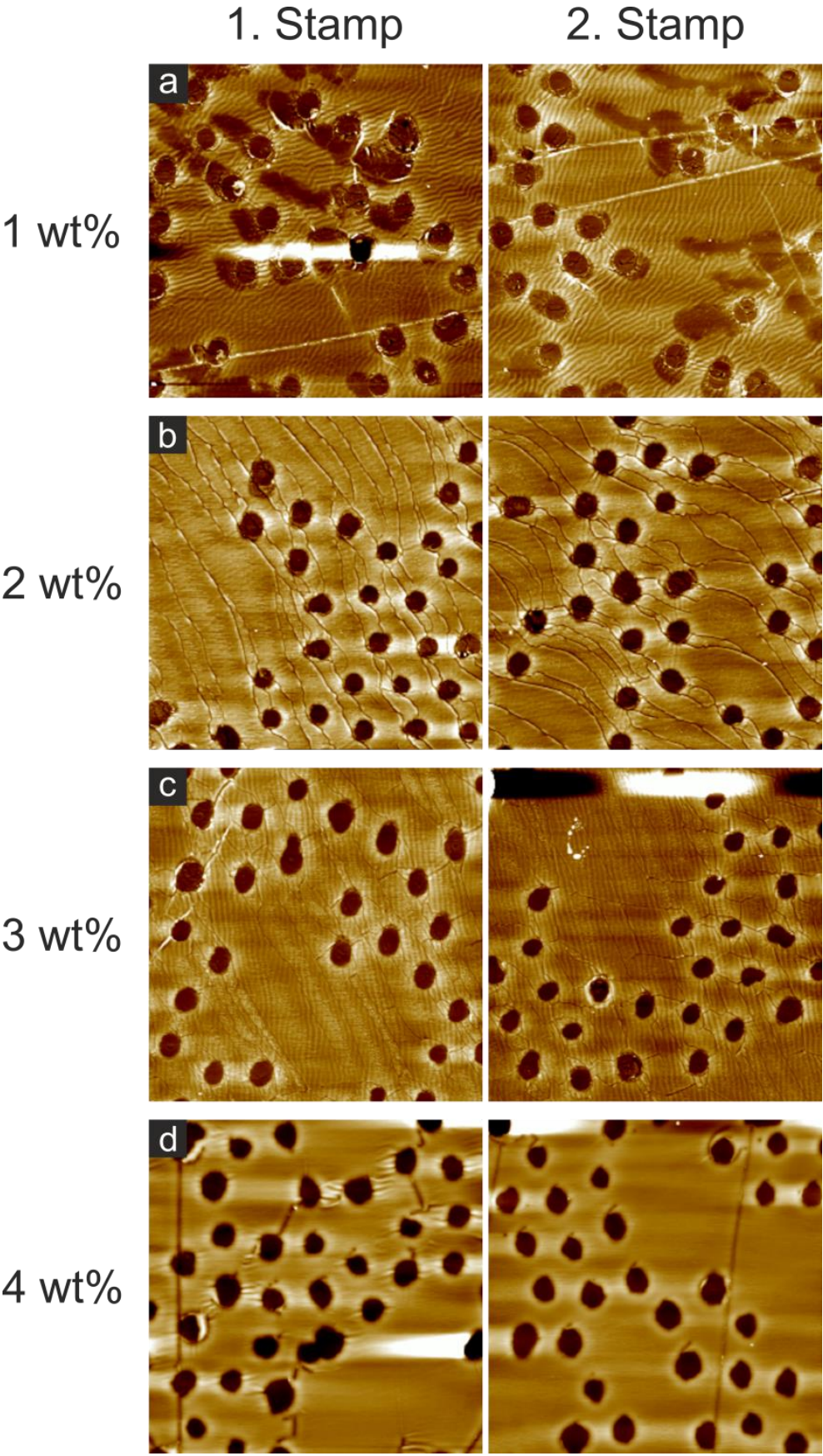
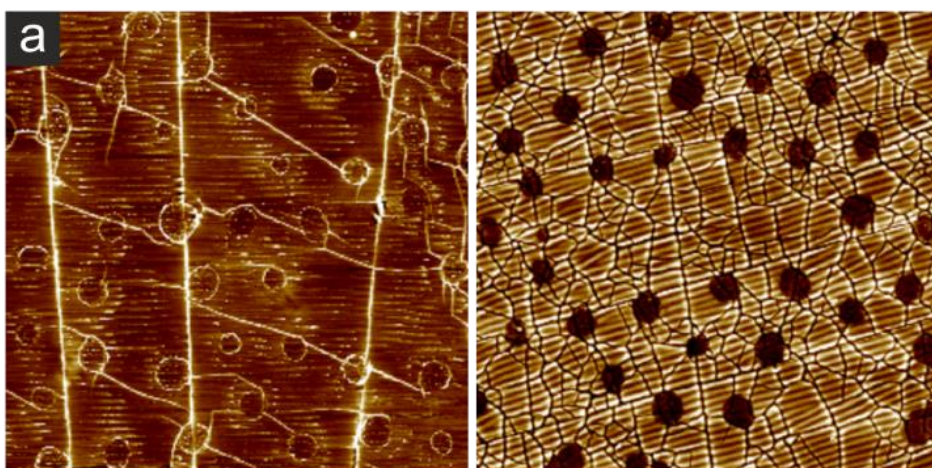


Figure S13 SFM images with a size of $(35 \times 35) \mu\text{m}^2$ of the first and second PDMS stamp after $5 \mu\text{m}$ DPP release: a) 1 wt% PEI - Height Scale 55 nm. b) 2 wt% PEI - Height Scale 60 nm. c) 3 wt% PEI - Height Scale 70 nm. d) 4 wt% PEI - Height Scale 180 nm.

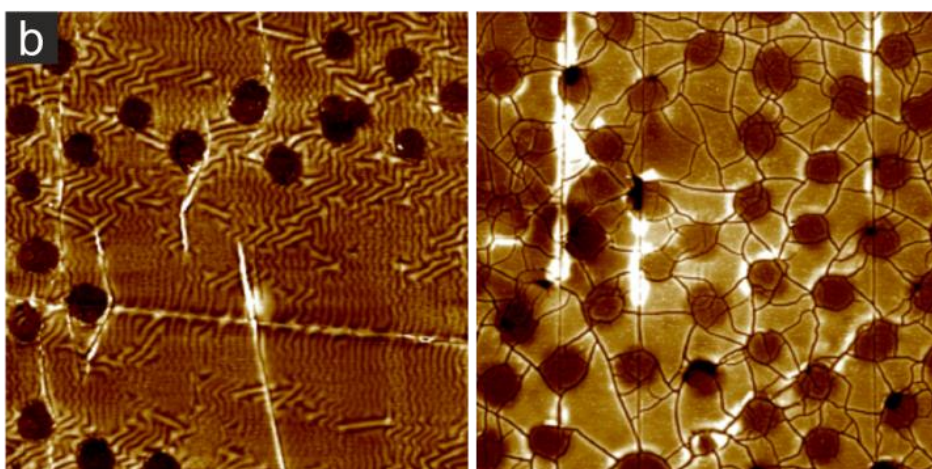
1. Stamp

2. Stamp

1 wt%



2 wt%



3 wt%

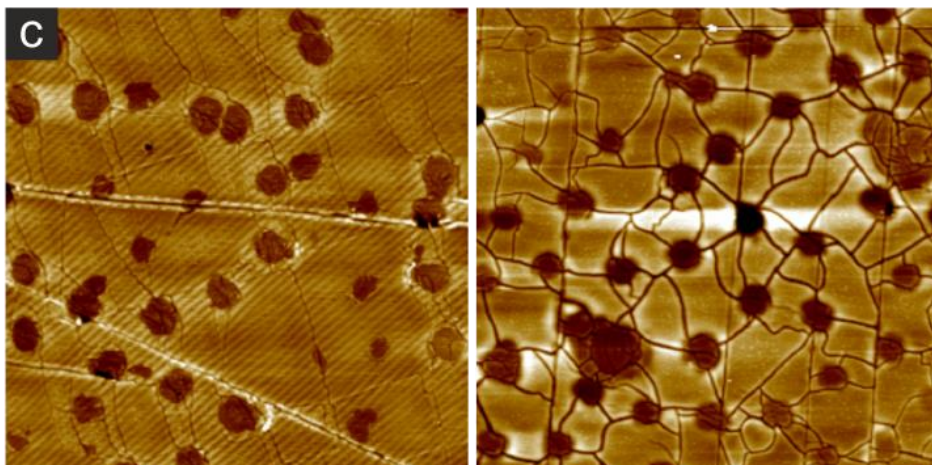


Figure S14 SFM images with a size of $(35 \times 35) \mu\text{m}^2$ of the first and second PDMS stamp after $4 \mu\text{m}$ DPP release: a) 1 wt% PEI - Height Scale 30 nm. b) 2 wt% PEI - Height Scale 70 nm. c) 3 wt% PEI - Height Scale 100 nm.

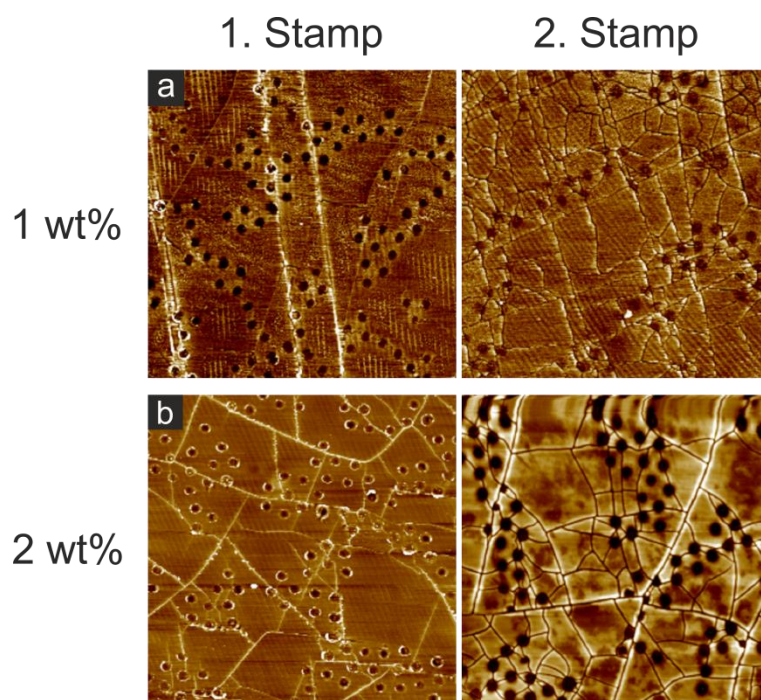


Figure S15 SFM images with a size of $(35 \times 35) \mu\text{m}^2$ of the first and second PDMS stamp after $2 \mu\text{m}$ DPP release: a) 1 wt% PEI - Height Scale 50 nm. b) 2 wt% PEI - Height Scale 70 nm.

Influence of Particle Size Distribution on Patch Diameter

To calculate the influence of the natural particle size distribution on the patch diameter we develop the following simple mathematical model: The particle is completely emerged into the polymer film on top of the PDMS stamp, which is not penetrable and does not bend (see Fig. S16a). This model is very simplified and will give an absolute minimum for the influence of the particle size distribution, since bending of the soft PDMS stamps is more than reasonable and will lead to an increase in patch diameter. By measuring the polymer film thickness for the used PEI solutions we obtained h for our samples.¹⁹ The particle radius r is taken from the manufacturers records and possesses a certain range (cv. = coefficient of variation = δ). Therefore we are able to use:

$$\begin{aligned}(r - h)^2 + x^2 &= r^2 \\ x^2 &= r^2 - (r - h)^2 \\ x &= \sqrt{r^2 - (r - h)^2} \\ x &= \sqrt{r^2 - r^2 + 2rh - h^2} \\ x &= \sqrt{2rh - h^2}\end{aligned}$$

With this we are able to calculate the patch diameter d as follows:

$$d = 2x = 2\sqrt{2(r \pm \delta)h - h^2}$$

Fig. S16b – e display our resulting graphs for the theoretical patch diameter as a function of the polymer film thickness for all particles sizes. We calculated this value for the average particle radius r (black dots) and its size variations by adding its upper and lower size distribution value δ to the particle radius (red area). For given values of h , corresponding to the used PEI solutions (coloured points), we calculated the discrepancy $e_{\pm\delta}$ between the achieved values for $d(r)$ and $d(r \pm \delta)$. Due to the curvature of the particles the value of $e_{+\delta}$ resembling the upper distribution limit exhibits a larger value. Therefore this value was chosen to be compared to the measured error margins for the patch diameter d by fluorescence microscope.

We used two standard deviations (2δ) for our calculation, which should include 95 % of all particles included in our samples. Depending on the size distribution of our acquired particles the influence of the particle size on the patch diameter can reach values up to 87 % (4 wt% on 4 μm particles).

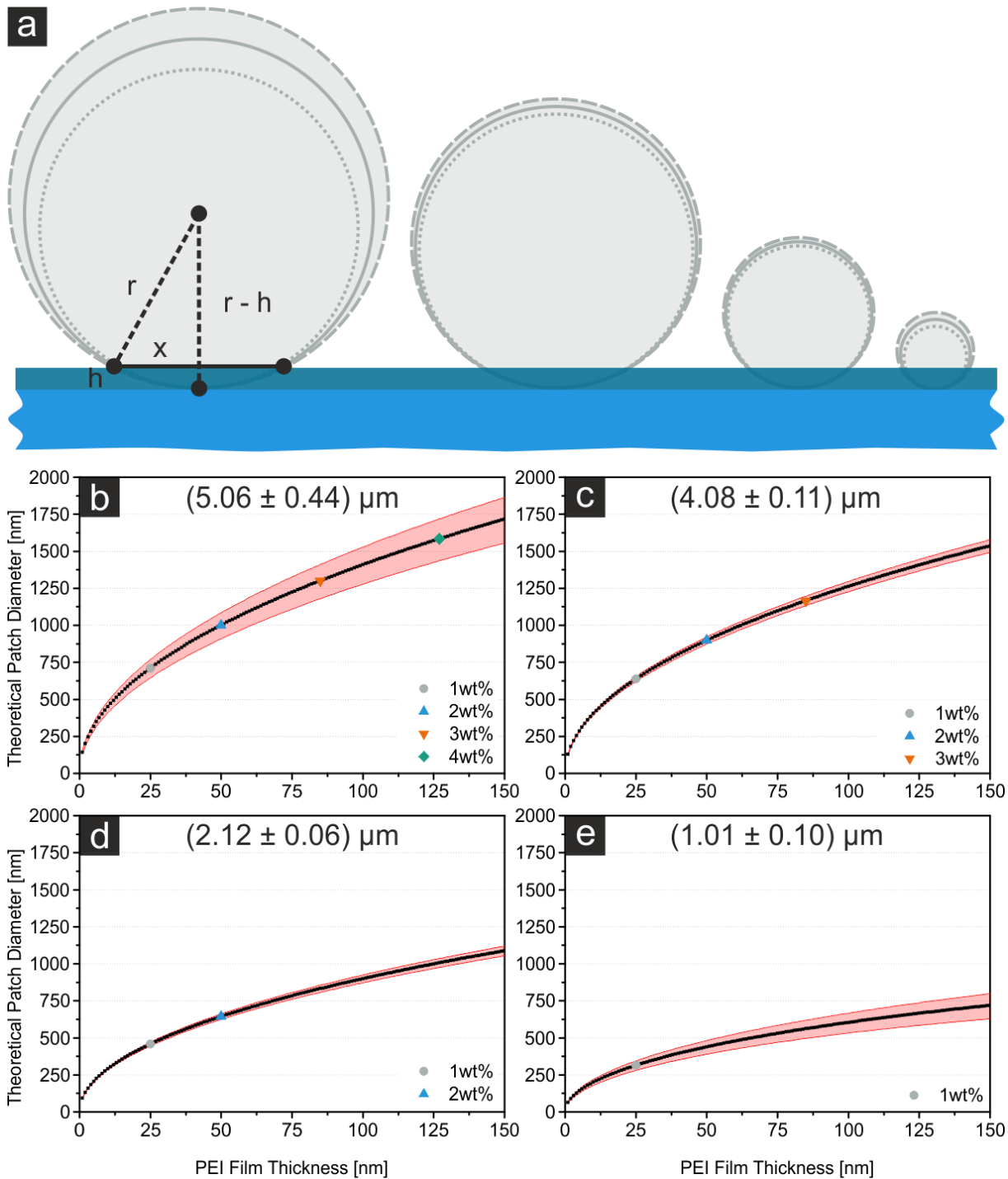


Figure S16 (a) Graphical illustration of the mathematical model to calculate the influence of the natural particle size distribution on the patch diameter during our microcontact printing. Used variables are the particle radius r , height of polymer film h and one half patch diameter x . (b–e) Theoretical patch diameter as a function of the polymer film thickness for $(5.06 \pm 0.44) \mu\text{m}$, $(4.08 \pm 0.11) \mu\text{m}$, $(2.12 \pm 0.06) \mu\text{m}$ and $(1.01 \pm 0.1) \mu\text{m}$ particles. Red areas highlight influence of the particle size distribution. Film thicknesses corresponding to the polymer solutions used experimentally are highlighted in different colours.

Electrostatic Bonding: pH Dependence

To proof the electrostatic interaction between the negative silica surface and the positively charged PEI, a microcontact printing sample, which was labelled using FITC, was divided into six equal portions. Every sample was centrifuged and dispersed into water with a certain pH. The pH values were adjusted prior using hydrochloric acid and ammonia. The samples were sonicated for 10 min and investigated using the fluorescence microscopy.

Between a pH of 4 to 10 no changes of the particle system could be observed. At a pH of 2 a detachment of the PEI patches from the silica surface was observable for most patches. Remarkably the detached patches did not lose their structure and were still observable using the fluorescence signal due to the FITC labelling. The same effect, but to an even stronger degree, was observable at a pH of 12. Almost all patches detached from the particles, but again were stable in solution without observable dissolving.

Reaching the isoelectric point (IEP) of silica at approx. 3.2 the negatively charged hydroxyl groups start to protonate, losing their charge. Therefore, the electrostatic bond breaks and the patches will be released. Reaching the IEP of polyethyleneimine the amine groups start to deprotonate. As before, the patches will be released due to the missing charge on the polymer. The stability of the patches in solution is explainable by the very high molecular weight of the used polyethyleneimine. Although the polymer should be water soluble, the strong entanglement after spin coating process between the long branched chains keeps the structure intact. Additionally, due to the protonated amine groups no charge repulsion among the polymer chains takes place, which would generally lead to a more stretched structure and therefore a better solubility in water. This experiment clearly shows the sole electrostatic bonding between the silica particles and the polyethyleneimine.

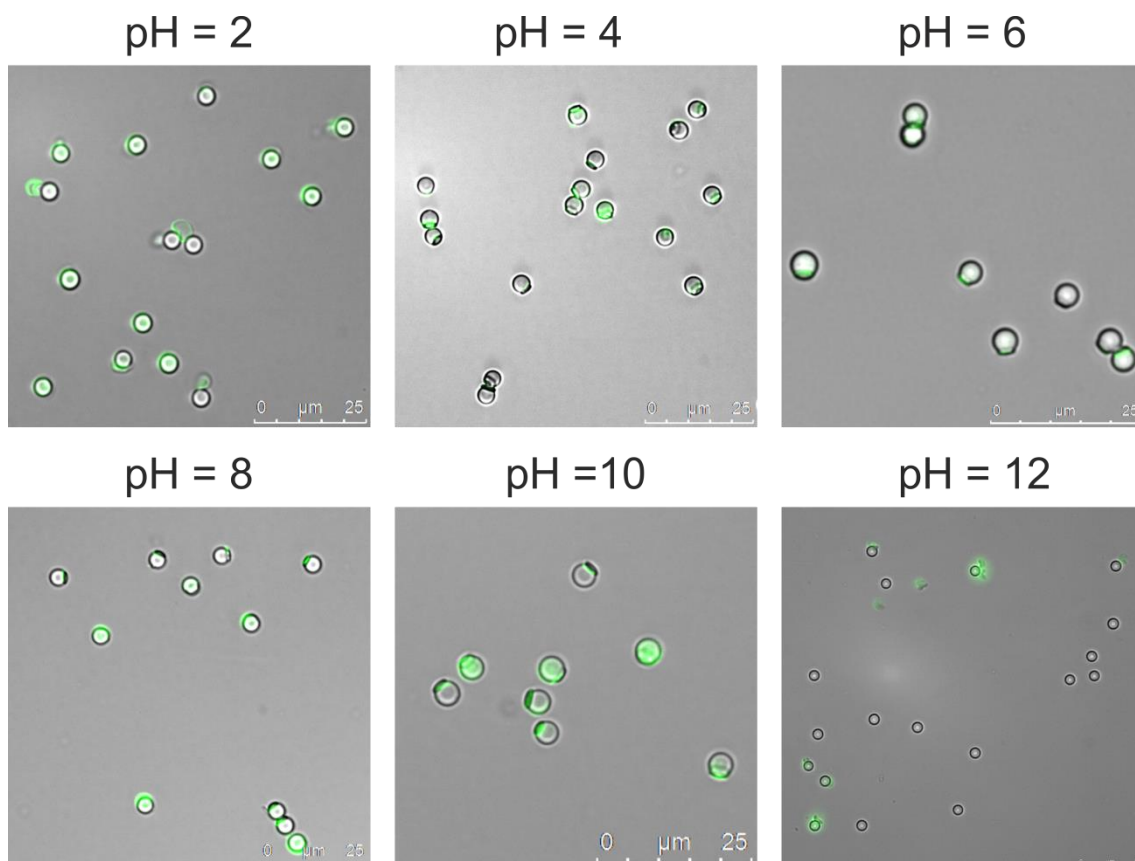


Figure S17 Fluorescence microscope pictures of single patched particles at different pH values ranging from 2 to 12. After passing the isoelectric point of silica (approx. 3.2) or polyethyleneimine (approx. 11) a detachment of the patches takes place.

Influence of Particle Size on Printing Pressure

To understand the decreasing patch thickness during the use of smaller particles, a simple mathematical calculation was conducted. For this, the particle radius r was converted into a particle area $A_{Particle}$ by using its two dimensional projection onto the substrate surface:

$$A_{Particle} = \pi * r^2$$

With $A_{Particle}$ the number of particles $n_{Particle}$ on a substrate of the size $1 \times 1 \text{ cm}^2$ was calculated. Furthermore, to take into account the two-dimensional close-packing of equal spheres, the corresponding factor was introduced¹:

$$n_{Particle} = \frac{\pi}{3\sqrt{2}} * \left(1\text{cm}^2 / A_{Particle}\right)^2$$

As we want to calculate a relative printing pressure difference for different sphere sizes, the patch diameter d_x was calculated for all sizes ($x \mu\text{m}$) using the previously introduced formula with a film thickness h of 25 nm:

$$d_x = 2\sqrt{2rh - h^2}$$

The contact area between the individual particle and polymer film A_{Patch} was approximated by:

$$A_{Patch} = \pi * \left(d_x/2\right)^2$$

With A_{Patch} and $n_{Particle}$ the total contact area C_x could be calculated:

$$C_x = A_{Patch} * n_{Particle}$$

Finally, with C_x and the printing force F_p , the printing pressure P_x for different particle sizes was calculated:

$$P_x = \frac{F_p}{C_x}$$

For better visualization a relative printing pressure P_r scaled to the printing pressure of the $5 \mu\text{m}$ silica particle sample was introduced:

$$P_r = \frac{P_x}{P_{5\mu\text{m}}} * 100\%$$

¹ J.L. Lagrange, *Nouv. Mem. Acad. Roy. Sc. Belle Lettres*, **1773**, 265-312.

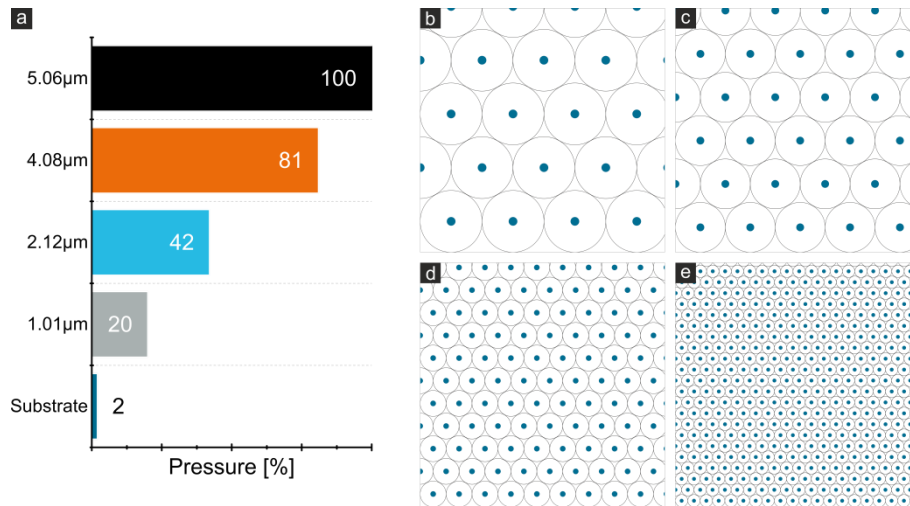


Figure S18 a) Diagram shows the relative printing pressure P , for different particle sizes and a flat substrate during microcontact printing at constant printing force. (b - e) Graphical illustration of the silica particle monolayer for different sphere sizes (5.06 μm , 4.08 μm , 2.12 μm , 1.01 μm). The blue coloured area displays the contact area of the individual particle surface with the underlying polymer layer with a thickness of 25 nm. This value was calculated by using the previously described formula.